

# Seismic Images of Crust and Upper Mantle Beneath Tibet: Evidence for Eurasian Plate Subduction

R. Kind,<sup>1,2\*</sup> X. Yuan,<sup>1</sup> J. Saul,<sup>1</sup> D. Nelson,<sup>3†</sup> S. V. Sobolev,<sup>1,4</sup> J. Mechie,<sup>1</sup> W. Zhao,<sup>5</sup> G. Kosarev,<sup>4</sup> J. Ni,<sup>6</sup> U. Achauer,<sup>7</sup> M. Jiang<sup>5</sup>

Seismic data from central Tibet have been combined to image the subsurface structure and understand the evolution of the collision of India and Eurasia. The 410- and 660-kilometer mantle discontinuities are sharply defined, implying a lack of a subducting slab beneath the plateau. The discontinuities appear slightly deeper beneath northern Tibet, implying that the average temperature of the mantle above the transition zone is about 300°C hotter in the north than in the south. There is a prominent south-dipping converter in the uppermost mantle beneath northern Tibet that might represent the top of the Eurasian mantle lithosphere underthrusting the northern margin of the plateau.

A number of international seismic experiments have been carried out in Tibet to unravel the structure of the crust and upper mantle below the high plateau (1–6) caused by the Indian-Eurasian continental collision. This collision, which has been ongoing

since 50 million years ago, forms the highest mountains and the biggest plateau on Earth and also deforms large parts of central and east Asia. We have combined all available high-quality teleseismic earthquake records and used the receiver func-

tion technique [see, e.g. (7, 8)] for constructing two crust-mantle cross sections through the plateau (Figs. 1 and 2, east and west lines). Seismic observations constraining the thickness of the crust in Tibet have been accruing for more than 20 years. Although it is generally accepted that the Tibetan crust is about double the normal thickness and that it thins somewhat toward the north (6, 9, 10), different authors using different techniques report variations of more than 20 km in the Moho depth at the same place [reviewed in (6)]. The receiver

<sup>1</sup>GeoForschungsZentrum Potsdam, Telegrafenberg, 14473 Potsdam, Germany. <sup>2</sup>Freie Universität Berlin, 12249 Berlin, Germany. <sup>3</sup>Department of Earth Sciences, Syracuse University, Syracuse, NY 13244, USA. <sup>4</sup>Institute of the Physics of the Earth, Russian Academy of Sciences, B. Gruzinskaya 10, 128810 Moscow, Russia. <sup>5</sup>Chinese Academy of Geological Sciences, 26 Baiwanzhang Road, Beijing 100037, China. <sup>6</sup>Department of Physics, New Mexico State University, Las Cruces, NM 88003, USA. <sup>7</sup>École et Observatoire des Sciences de la Terre, Université Louis Pasteur, 5 rue René Descartes, F-67084 Strasbourg Cedex, France.

\*To whom correspondence should be addressed. E-mail: kind@gfz-potsdam.de  
†Deceased (18 August 2002).

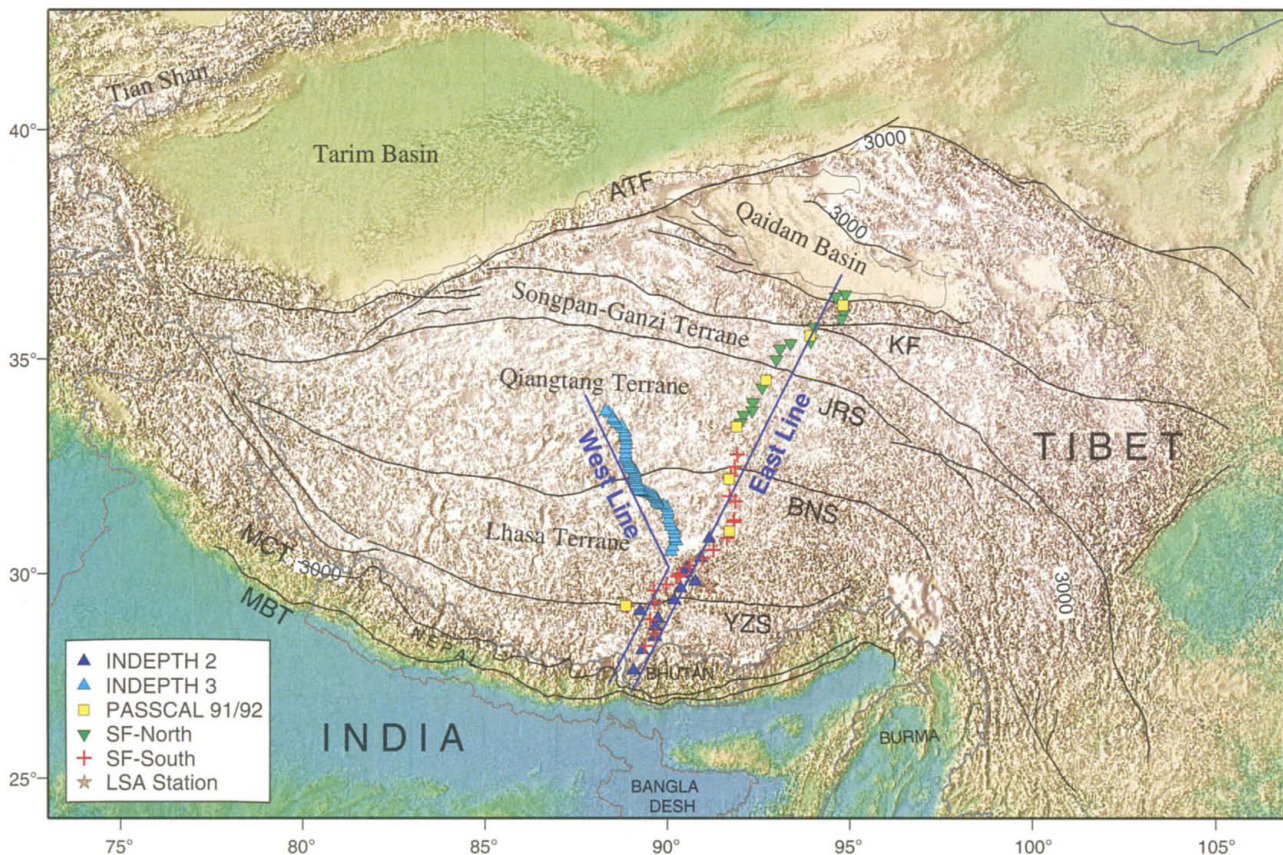


**Fig. 1.** Station locations on the topographic map of Tibet (3000 m elevation is marked). Stations of different experiments are marked by different symbols. [PASSCAL 91/92 (1), SF-North (5), SF-South (2), LSA—seismic station at Lhasa]. Solid lines represent the important structural boundaries: MBT (Main Himalaya Thrust), MCT (Main Central

Thrust), YZS (Yarlung-Zangbo suture), BNS (Bangong-Nujiang suture), JRS (Jinsha River suture), KF (Kunlun Fault), and ATF (Altyn Tagh Fault). These boundaries divide Tibet into several terranes. The stations are divided into two profiles (west and east lines).

function data provide a uniform and densely sampled observation of the Moho depth and the average crustal ratio of compressional and shear velocities ( $V_p/V_s$ ) across much of the plateau.

On both east and west sections (Fig. 3) (11), the Moho imaged in the direct conversion ( $Pms$ ) as well as in the two multiple phases is similar in depth and reflection character. This is also true of the distinct lower crustal “doublet” in the south (12). There are, however, discrepancies in the Moho depths imaged in the direct conversion versus the multiples between 30° and 32°N on the east line and between 32° and 34°N on the west line. In these areas the crustal  $V_p/V_s$  ratio is different from the ratio of 1.75 used in the migrations. The images in Fig. 3 and fig. S1 show that the Tibetan crust varies in thickness from a maximum of about  $78 \pm 3$  km to a minimum of about  $65 \pm 3$  km. The maximum thickness occurs within the Lhasa terrane about 100 km north of the Yarlung-Zangbo suture ( $\sim 30^\circ N$ ). Immediately to the north, the Moho shallows to its minimum depth over a distance of 50 to 100 km (west and east lines, respectively) and then maintains a roughly constant depth to the northern margin of the plateau ( $\pm$  few km). There is no evidence of fault offsets in the Moho beneath the surface traces of the Yarlung-Zangbo and Bangong-Nujiang sutures. The thinning of the crust beneath the northern Lhasa terrane coincides with the position of the hypothesized India-Asia mantle suture (8, 13). A displacement of the Moho (2 to 3 km) is also imaged beneath the surface trace of the Jinsha River suture. This may reflect Cenozoic transpressional reactivation of the originally Triassic age structure (5). The crustal  $V_p/V_s$  is anomalously high within the Lhasa terrane, beneath the northern Yadong-Gulu rift (Fig. 3E). This is one of the more prominent north-trending active rifts in Tibet and shows evidence of magma and/or fluids in the underlying crust (3).

Our results suggest that there is no substantial regional difference in crustal  $V_p/V_s$  between northern and southern Tibet. Over most of the plateau, the amount of magma and/or fluid in the crust is not great enough to elevate average crustal  $V_p/V_s$ , even though the magma and/or fluid is great enough to enhance the electrical conductivity of the plateau (14). Taken together with experimental results on the electrical properties of rocks undergoing melting (15), these observations imply that, regionally, the melt/fluid in the Tibetan crust is probably on the order of a few percent (15). Within the crust beneath the active Tibetan rifts, however, there are apparently locally larger accumulations of melt/fluid, which

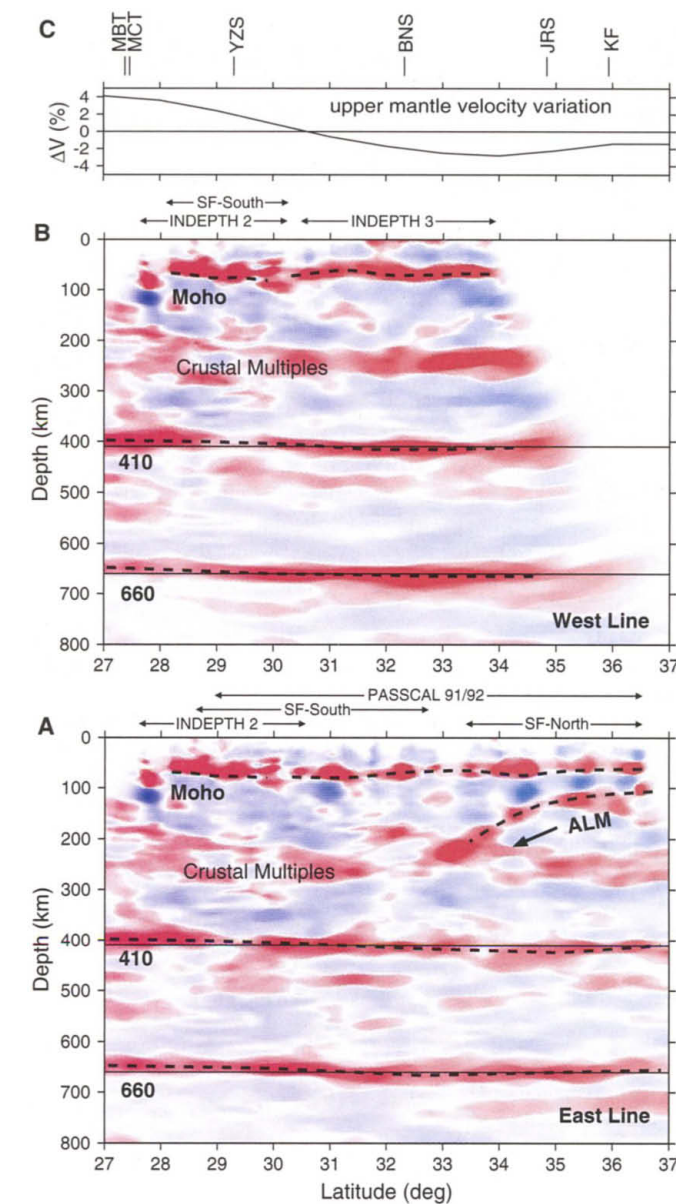


**Fig. 2.** Migrated receiver function data along two sections (locations are shown in Fig. 1). The east section (A), located along the Lhasa-Golmud highway, includes data from all experiments except INDEPTH 3. The west section (B) shows the data of INDEPTH 3 plus the southernmost part of the east line. Positive amplitudes are plotted in red, negative in blue. The main conversion boundaries have been marked and labeled as follows: Moho (the crust-mantle boundary), 410 and 660 (the upper mantle discontinuities), and ALM (detached Asian lithospheric mantle). Crustal multiples reverberate between the Moho and the surface. (C) Percentage of the northerly decreasing S wave velocity in the upper mantle above 410 km depth, which causes the apparent north-dipping of the 410 and 660.

are large enough to perturb the average crustal  $V_p/V_s$ .

The 410- and 660-km velocity discontinuities marking the top and bottom of the mantle transition zone are well imaged beneath Tibet on the two profiles (Fig. 2). These velocity discontinuities are thought to mark mineralogic phase changes within the mantle: the 410-km discontinuity marking the transformation from olivine to  $\alpha$ -spinel, and the 660-km discontinuity marking the transition from  $\beta$ -spinel to perovskite + magnesiowüstite (16). Experimental studies have shown that both reactions are sensitive to temperature and have Clapeyron slopes of opposite signs. In the absence of other effects, a lateral increase in temperature at the level of the transition zone should be reflected in a deepening of the 410-km discontinuity and a shallowing

of the 660-km discontinuity (and vice versa). The expected magnitude of the effect is about 100°C per 10 km thickness change of the transition zone (16). On our east and west sections in Tibet, the 410- and 660-km discontinuities are imaged with a constant separation across the profiles. This implies that any north-south variation in the temperature of the mantle within the transition zone must be less than about  $\pm 50^\circ C$ . Although the two discontinuities are parallel across the profiles, both are depressed by about 20 km beneath the northern plateau relative to the south. The deeper discontinuities imply that there is a south-to-north decrease in the average shear-wave velocity of the upper mantle of about 5%. This can be explained by a northward increase in the average temperature between the surface and 410 km depth of about 300°C (17–19).

REPORTS

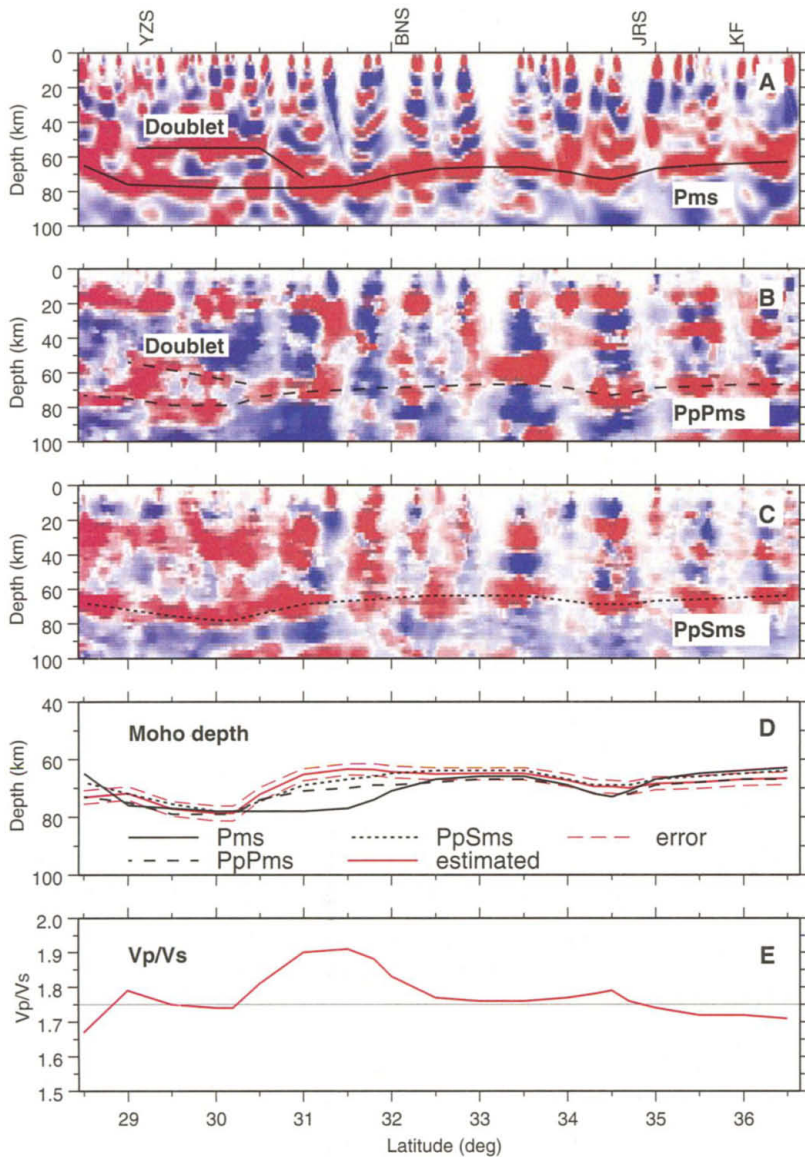


**Fig. 3.** Crustal section of the east line across the Tibetan plateau migrated by directly converted phases (*Pms*) (A) and two multiples (*PpPms*, *PpSms*) (B and C). Average crustal  $V_p$  of 6.2 km/s is used. The Moho imaged with each phase is marked in the corresponding panel. In each panel the energy from the indicated phase should, in principle, have migrated correctly, whereas all other energy should be mispositioned. If there are no lateral variations in crustal  $V_p/V_s$ , the images generated by each phase should mimic each other. Note that a lower crustal phase at the Yarlung-Zangbo suture (marked Doublet) is visible in the direct conversion (A) and the *PpSms* multiple (B). (D and E) The north-south variation of the Moho observed in the three seismic phases, and the calculated variation of Moho depth and  $V_p/V_s$  ratio. Previous seismic experiments have shown that average crustal  $V_p$  in Tibet is in the range 6.0 to 6.4 km/s [slow relative to stable continental regions (6, 25, 26)]. The dashed red bounds show the effect of a variation of  $\pm 0.2$  km/s in crustal  $V_p$ .

The continuity and the constant separation of the 410- and 660-km interfaces implies that there is no lithosphere slab penetrating the mantle transition zone beneath Tibet. This would require that the Indian plate currently underthrusting southern Tibet be detached from whatever oceanic lithosphere preceded it northward in the collision with the Eurasian plate. The high-velocity Tethyan slab identified in global seismic tomographic inversions pro-

jecting to the surface beneath peninsular India (20, 21) is a possible candidate. In this scenario, the Tethyan (Neotethyan) oceanic slab would have detached from the northern margin of India early in the collision and then would have been overridden by India as it continued northward.

Our east section confirms, as imaged previously by (8), the existence of the south-dipping interface beneath northern Tibet (ALM, Fig. 2A). This feature is trace-

able southward from about 100 km depth beneath the Kunlun fault to about 250 km depth beneath the center of the Qiangtang terrane, where it becomes obscured by multiple reflections within the crust. We speculate, in accordance with previous work (22, 23), that it is the manifestation of southward-dipping Eurasian plate (Qaidam basin) mantle lithosphere underthrusting northern Tibet. Our sections do not show obvious evidence for a north-dipping interface beneath southern Tibet as imaged by (8). This seems to support the older tectonic interpretation (9, 10) that Indian continental lithosphere has underthrust beneath Tibet subhorizontally to about the middle of the plateau and that it has a broken, northern edge that is almost vertical. However, it may also be that the north-dipping boundary exists but the seismic velocity contrast at this boundary is too small to be stably imaged by the receiver functions with the data available.

References and Notes

1. T. J. Owens, G. E. Randall, F. T. Wu, R. Zeng, *Bull. Seismol. Soc. Am.* **83**, 1959 (1993).
2. A. Hirn et al., *Nature* **375**, 571 (1995).
3. K. D. Nelson et al., *Science* **274**, 1684 (1996).
4. R. Kind et al., *Science* **274**, 1692 (1996).
5. G. Wittlinger et al., *Earth Planet. Sci. Lett.* **139**, 263 (1996).
6. W. Zhao et al., *Geophys. J. Int.* **145**, 486 (2001).
7. X. Yuan, J. Ni, R. Kind, J. Mechie, E. Sandvol, *J. Geophys. Res.* **102**, 27491 (1997).
8. G. Kosarev et al., *Science* **283**, 1306 (1999).
9. P. Molnar, *Philos. Trans. R. Soc. London Ser. A* **326**, 33 (1988).
10. T. J. Owens, G. Zandt, *Nature* **387**, 37 (1997).
11. See supporting data on Science Online.
12. This feature probably marks the top of a high-velocity lower crustal layer also observed beneath southern Tibet on refraction data (24).
13. Y. Jin, M. K. McNutt, Y. Zhu, *J. Geophys. Res.* **101**, 11275 (1996).
14. W. Wei et al., *Science* **292**, 716 (2001).
15. G. M. Partzsch, F. R. Schilling, J. Arndt, *Tectonophysics* **317**, 189 (2000).
16. G. Helffrich, *Rev. Geophys.* **38**, 141 (2000).
17. S. Karato, *Geophys. Res. Lett.* **20**, 1623 (1993).
18. S. V. Sobolev et al., *Earth Planet. Sci. Lett.* **139**, 147 (1996).
19. S. V. Sobolev et al., *Tectonophysics* **275**, 143 (1997).
20. S. P. Grand, R. D. van der Hilst, S. Widiyantoro, *Geol. Soc. Am. Today* **7**, 1 (1997).
21. R. van der Voo, W. Spakman, H. Bijwaard, *Earth Planet. Sci. Lett.* **171**, 7 (1999).
22. S. D. Willett, C. Beaumont, *Nature* **369**, 642 (1994).
23. P. Tapponnier et al., *Science* **294**, 1671 (2001).
24. A. Hirn et al., *Nature* **307**, 23 (1984).
25. A. J. Rodgers, S. Y. Schwartz, *Geophys. Res. Lett.* **24**, 9 (1997).
26. ———, *J. Geophys. Res.* **103**, 7137 (1998).
27. Project INDEPTH is supported by the Deutsche Forschungsgemeinschaft, the German Bundesministerium für Bildung und Wissenschaft, NSF (USA), and the Ministry of Land and Resources of China. Instruments were provided by IRIS-PASSCAL and the GFZ Potsdam geophysical instrument pool.

Supporting Online Material

www.sciencemag.org/cgi/content/full/298/5596/1219/DC1  
Materials and Methods  
Figs. S1 to S3

5 September 2002; accepted 30 September 2002